DALTON
FULL PAPER

Hydrothermal syntheses and crystal structures of two-dimensional (2D) layered vanadium oxide complexes: $M(bipy)(H_2O)V_2O_6$ (M = Ni, Co, bipy = bipyridine) and $[Ni(bipy)_2V_6O_{17}]$†

Cai-Ming Liu,[a,b] Song Gao,*[a] Huai-Ming Hu,[b] Xianglin Jin[a] and Hui-Zhong Kou[a]

[a] *College of Chemistry and Molecular Engineering, State Key Laboratory of Rare Earth Materials Chemistry and Applications, Peking University, Beijing 100871, P. R. China. E-mail: gaosong@pku.edu.cn*

[b] *Organic Solids Laboratory, Center for Molecular Science, Institute of Chemistry, Chinese Academy of Sciences, Beijing 100080, P. R. China*

Received 28th June 2001, Accepted 14th November 2001
First published as an Advance Article on the web 28th January 2002

Double layered vanadium oxide metal coordination complexes, $[Ni(bipy)(H_2O)V_2O_6]_\infty$ **1** and $\{[Ni(bipy)_2]_2V_6O_{17}\}_\infty$ **2**, have been isolated from the same hydrothermal reaction container. X-Ray crystallography shows that **1** consists of unique two-dimensional layers constructed from a vanadium oxide chain $\{V_2O_6\}_n^{2n-}$ and covalently linked by $Ni(bipy)(H_2O)^{2+}$ subunits. In contrast **2** and the previously reported $Zn(bipy)_2V_6O_{17}$ are isomorphic compounds. Only $[Co(bipy)(H_2O)V_2O_6]_\infty$, **3**, was obtained when cobalt was substituted for nickel in a similar reaction, and X-ray diffraction analysis reveals that the topology of **3** is essentially identical to that of **1**. The magnetic behavior of **1** and **2** suggests a dominant single ion effect with only very weak magnetic interactions.

Recently, the use of organic amines as structural directors for the fabrication of organic–inorganic hybrid materials has attracted great interest in the research fields of catalysis, molecular adsorption, electromagnetism and photochemistry.[1] Furthermore, transition metal complexes have also been found to serve as binders of vanadium oxide frameworks.[2–6] Examples explored include discrete clusters, one-dimensional (1D) chains and two-dimensional (2D) layer structures. Most layered vanadium solid state complexes show three-dimensional-like framework compositions and possess mixed valence characteristics,[2a,3] and all 1D chain vanadium oxide metal coordination complexes $Cu(NH_3)_2V_2O_6$,[5] $Cu(dien)V_2O_6{\cdot}H_2O$,[4] $Cu(en)V_2O_6$,[2c] $Cu(bipy)V_2O_6$,[2c] $Cu(bipy)_2V_2O_6$,[2c] and [(2,2′-biphen)Co]$V_3O_{8.5}$[6b] (dien = diethylenetriamine, en = ethylenediamine, 2,2′-biphen = 2,2′-biphenanthroline) exhibit the same vanadium oxide chain $\{V_2O_6\}_n^{2n-}$ to which coordination groups are attached. On the other hand, small changes of hydrothermal parameters such as time, temperature, stoichiometry, pH and reaction duration have a great influence on the reaction outcome. Several pathways are available under non-equilibrium crystallization conditions but metastable kinetic phases are most likely to be isolated rather than the thermodynamic phase.[7] In this paper, we present a rare example where two stable phases, $[Ni(bipy)(H_2O)V_2O_6]_\infty$ **1** and $\{[Ni(bipy)_2]_2V_6O_{17}\}_\infty$ **2**, are isolated from the same hydrothermal reaction container. Although **2** possesses a structure isomorphous with $Zn(bipy)_2V_6O_{17}$,[2a] complex **1** exhibits a unique layered structure where vanadium oxide chains $\{V_2O_6\}_n^{2n-}$ are incorporated by $Ni(bipy)(H_2O)^{2+}$ subunits to form a novel two-dimensional (2D) topology. Interestingly, only $[Co(bipy)(H_2O)V_2O_6]_\infty$ **3**, which is isomorphous with **1**, was obtained when $Co(NO_3)_2$ took the place of $Ni(NO_3)_2$ as one of the starting materials.

† Electronic supplementary information (ESI) available: figures showing fragments of the net comprising complexes **1** and **3** and a basic layer unit of complex **2**. See http://www.rsc.org/suppdata/dt/b1/b105700f/

Experimental

Materials and methods

All chemicals were purchased from commercial sources and used without further purification. Elemental analyses of carbon, hydrogen and nitrogen were carried out with an Elementar Vario EL. The infrared spectroscopy on KBr pellets was performed on a Magna-IR 750 spectrophotometer in the region of 4000–400 cm^{-1}. Variable-temperature magnetic susceptibility measurements for **1** and **2** were performed on a Maglab System[2000] magnetometer. Effective magnetic moments were calculated by the equation $\mu_{eff} = 2.828(\chi_M T)^{1/2}$, where χ_M is the molar magnetic susceptibility. The experimental susceptibilities were corrected for the diamagnetism of the constituent atoms (Pascal's Tables).[8]

Preparation of complexes

$[Ni(bipy)(H_2O)V_2O_6]_\infty$ 1 and $\{[Ni(bipy)_2]_2V_6O_{17}\}_\infty$ 2. A mixture of NH_4VO_3 (1.0 mmol), H_3BO_3 (1.5 mmol), $Ni(NO_3)_2{\cdot}6H_2O$ (1 mmol), 2,2′-bipy (2 mmol) and H_2O (15 ml) was stirred for 20 min. The mixture was then transferred to a Teflon-lined stainless steel autoclave (25 ml) and kept at 160 °C for 4–5 days. After slow cooling, crystalline samples of **1** and **2** were manually selected as green (30% yield) and dark brown (20% yield) blocks, respectively. Attempts to prepare monophasic materials failed. However, the yield of **2** relative to **1** was improved when a longer time was used. A similar trend has also been reported quite recently for the synthesis of $[Cu(tepy)MoO_4]{\cdot}3H_2O$ and $[Cu(tepy)Mo_2O_7]$ (tepy = 2,2′:6′2″-terpyridyl).[9] Anal. calc. for $C_{10}H_{10}N_2O_7NiV_2$ **1**: C, 27.88; H, 2.34; N, 6.50%; Found: C, 27.65; H, 2.45; N, 6.30%. For $C_{20}H_{16}N_4O_{8.5}NiV_3$ **2**: C, 36.40; H, 2.44; N, 8.49%; Found: C, 36.32; H, 2.52; N, 8.34%. IR (KBr, cm^{-1}) for **1**: 1673(w), 1621(w), 1599(m), 1490(w), 1472(w), 1442(m), 1318(w), 1250(w), 1154(w), 1058(w), 1028(w), 966(s), 911(s), 885(s), 848(s), 774(m), 738(m), 655(vs), 560(w); for **2**: 1641(w), 1599(m), 1574(w), 1493(w), 1473(w), 1444(m), 1315(w), 1250(w), 1161(w),

 DOI: 10.1039/b105700f

Table 1 Crystal data for complexes **1**, **2** and **3**

	1	**2**	**3**
Formula	$C_{10}H_{10}N_2O_7NiV_2$	$C_{20}H_{16}N_4O_{8.5}NiV_3$	$C_{10}H_{10}N_2O_7CoV_2$
M	430.79	659.90	431.01
T/K	293(2)	293(2)	293(2)
Crystal system	Orthorhombic	Monoclinic	Orthorhombic
Space group	*Pca*2(1)	*P*2(1)/*C*	*Pca*2(1)
a/Å	9.171(2)	15.503(3)	9.212(2)
b/Å	10.514(2)	14.748(3)	10.543(2)
c/Å	14.339(3)	10.467(2)	14.388(3)
β/°	90	92.01(3)	90
V/Å^3	1382.6(5)	2391.7(8)	1397.4(5)
Z	4	4	4
D_c/g cm^{-3}	2.070	1.833	2.049
μ(Mo-Kα)/mm^{-1}	2.707	1.968	2.518
Reflections collected	1646	5474	1633
Independent reflections	1580	3589	1590
Final $R1$, $wR2$ [$I > 2\sigma$]	0.0171, 0.0369	0.0276, 0.0673	0.0167, 0.0347

1060(w), 1024(w), 981(m), 951(s), 904(m), 876(w), 834(m), 771(m), 742(m), 659(vs), 560(w).

$[Co(bipy)(H_2O)V_2O_6]_\infty$ 3. A mixture of NH_4VO_3 (1.0 mmol), H_3BO_3 (1.5 mmol), $Co(NO_3)_2{\cdot}6H_2O$ (1 mmol), 2,2′-bipy (2 mmol) and H_2O (15 ml) was heated at 160 °C in a Teflon-lined stainless steel autoclave (25 ml) for 5 days, yielding black brown rods along with some unidentified thin yellow rods. The black brown rod-like crystals of **3** were picked for the analysis in *ca.* 30% yield. Anal. calc. for $C_{10}H_{10}N_2O_7CoV_2$ **3**: C, 27.87; H, 2.34; N, 6.50%; Found: C, 27.61; H, 3.57; N, 6.23%. IR (KBr, cm^{-1}): 1605(w), 1497(w), 1448(m), 1311(w), 1250(w), 1177(w), 1161(w), 1111(w), 1021(w), 958(m), 923(s), 915(s), 839(s), 800(w), 778(m), 756(w), 726(w), 706(w), 637(vs), 538(w).

Crystallography

Crystal data for complexes **1**–**3** were collected using the Rigaku RAXIS RAPID IP imaging plate system. The data were corrected for Lorentz-polarization effects and absorption corrections were applied. All of the non-hydrogen atoms were refined anisotropically and all of the hydrogen atoms were generated geometrically and allowed to ride on their parent carbon atoms. The structures were solved by direct methods and refined using SHELXL 97.[10] Crystal data, data collection and refinement parameters for complexes **1**–**3** are given in Table 1, with selected bond lengths and angles in Tables 2–4.

CCDC reference numbers 173604–173606.

See http://www.rsc.org/suppdata/dt/b1/b105700f/ for crystallographic data in CIF or other electronic format.

Results and discussion

Crystal structures of 1 and 3

The crystal structure of **1** consists of 1D corner-sharing tetrahedral $(VO_3)_n^{2n-}$ chains running along the *a* axis, linked through Ni(bipy)$(H_2O)^{2+}$ fragments *via* oxygen atoms into a 2D covalent network (Fig. 1, Table 2). There are two crystallographically independent vanadium atoms V1 and V2, which are corner-shared by O3 and O4 atoms. Both V1 and V2 sites are covalently attached: the V1 atom binds one Ni(bipy)-$(H_2O)^{2+}$ fragment through O1 atom whereas the V2 atom binds two Ni(bipy)$(H_2O)^{2+}$ fragments through O5 and O6 atoms, consequently, the terminal vanadyl (V=O) group is found only in the V1 site though the V2 site shows VO_4 tetrahedral geometry too. To the best of our knowledge, this feature is unique, the terminal vanadyl (V=O) groups are always present in *all* vanadium sites in other reported vanadium solid-state complexes.[2–6]

The nickel atom, which has a slightly distorted octahedral geometry, is coordinated by one 2,2′-bipy ligand and one water molecule, with Ni(bipy)$(H_2O)^{2+}$ fragments further covalently attached to neighboring $(VO_3)_n^{2n-}$ chains through O1, O5, O6 or their symmetry equivalents. Within each NiVO layer there are alternately arranged six- and four-membered rings. The six-membered ring is defined by four VO_4 tetrahedra and two NiN_2O_3Ow octahedra, whereas the four-membered ring is defined by three VO_4 tetrahedra and one NiN_2O_3Ow octahedron. Each six-membered ring shares two edges with two adjacent six-membered rings and four edges with four neighboring four-membered rings, and each four-membered ring shares all edges with four six-membered rings to form a unique 2D topology.

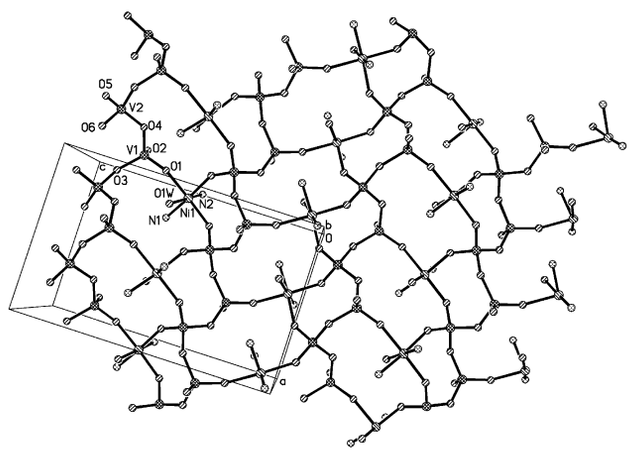

Fig. 1 The structure of **1** viewed along the *b*-axis showing the layer constructed of 4,6-net sheets. All the C and H atoms are omitted for clarity.

The crystal structure of **3** shows the same topology as **1** (Fig. 2, Table 3), a similar 2D topology was only found in our recently reported coordination polymer $[NdM(bpym)(H_2O)_4(CN)_6]{\cdot}3H_2O$ (M = Fe and Co, bpym = 2,2′-bipyrimidine).[11] To our knowledge, **1** and **3** are the first examples of 2D layered vanadium oxide metal coordination complexes constructed of 4,6-net sheets. The Co–N bond distances (average 2.113 Å) are slightly larger than the Ni–N bond distances (average 2.064 Å) in **1** whereas the N1–Co1–N2 bond angle [77.58(9)°] is smaller than the N1–Ni1–N2 bond angle in **1** [79.56(9)°] (Tables 2 and 3). The Co1–O1w bond distance [2.166(2) Å] of **3** is slightly longer than the Ni1–O1w bond distance [2.108(2) Å] of **1**, and the V=O bond lengths in both **1** and **3** [1.608(2) and 1.6075(19) Å, respectively] are comparable.

Crystal structure of 2

The complex **2** was found to co-crystallize with **1**. When viewed down the *a*-axis, the crystal structure of **2** is seen to be con-

Table 2 Selected bond lengths (Å) and angles (°) for complex **1**

Ni1–O6$^{\#1}$	2.036(2)	Ni1–O5$^{\#2}$	2.041(2)
Ni1–N2	2.047(2)	Ni1–O1	2.062(2)
Ni1–N1	2.081(2)	Ni1–O1w	2.108(2)
V1–O2	1.608(2)	V1–O1	1.632(3)
V1–O3	1.802(2)	V1–O4	1.8279(19)
O6$^{\#1}$–Ni1–O5$^{\#2}$	91.55(9)	O6$^{\#1}$–Ni1–N2	93.04(9)
O5$^{\#2}$–Ni1–N2	93.52(9)	O6$^{\#1}$–Ni1–O1	172.96(9)
O5$^{\#2}$–Ni1–O1	87.37(9)	N2–Ni1–O1	93.97(9)
O6$^{\#1}$–Ni1–N1	93.61(9)	O5$^{\#2}$–Ni1–N1	171.57(9)
N2–Ni1–N1	79.56(9)	O1–Ni1–N1	88.30(9)
O6$^{\#1}$–Ni1–O1w	89.19(9)	O5$^{\#1}$–Ni1–O1w	92.30(9)
N2–Ni1–O1w	173.71(10)	O1–Ni1–O1w	83.90(9)
N1–Ni1–O1w	94.43(9)	O2–V1–O1	111.06(14)

Symmetry codes: #1 $-x, -y, z + 1/2$; #2 $-x + 1/2, y, z + 1/2$.

Table 3 Selected bond lengths (Å) and angles (°) for complex **3**

Co1–O5$^{\#3}$	2.0555(19)	Co1–O6$^{\#4}$	2.058(2)
Co1–O1	2.078(2)	Co1–N1	2.096(2)
Co1–N2	2.129(2)	Co1–O1w	2.166(2)
V1–O2	1.6075(19)	V1–O1	1.634(2)
O5$^{\#3}$–Co1$^{\#4}$–O6	92.32(8)	O5$^{\#3}$–Co1–O1	88.08(8)
O6$^{\#4}$–Co1–O1	171.78(8)	O5$^{\#3}$–Co1–N1	94.65(9)
O6$^{\#4}$–Co1–N1	94.23(8)	O1–Co1–N1	93.93(9)
O5$^{\#3}$–Co1–N2	171.01(8)	O6$^{\#4}$–Co1–N2	92.76(8)
O1–Co1–N2	87.95(8)	N1–Co1–N2	77.58(9)
O5$^{\#3}$–Co1–O1w	92.75(9)	O6$^{\#4}$–Co1–O1w	87.80(8)
O1–Co1–O1w	83.97(9)	N1–Co1–O1w	172.24(9)
N2–Co1–O1w	94.85(9)	O2–V1–O1	110.84(12)

Symmetry codes: #3 $-x, -y, z + 1/2$; #4 $-x + 1/2, y, z + 1/2$.

Table 4 Selected bond lengths (Å) and angles (°) for complex **2**

Ni1–O2	2.0255(17)	Ni1–N1	2.0553(19)
Ni1–N4	2.0614(19)	Ni1–N2	2.079(2)
Ni1–O7	2.0820(17)	Ni1–N3	2.127(2)
V2–O5	1.577(2)	V1–O1	1.6065(16)
V3–O3	1.610(2)		
O2–Ni1–N1	93.72(7)	O2–Ni1–N4	90.42(8)
N1–Ni1–N4	170.43(8)	O2–Ni1–N2	172.58(7)
N1–Ni1–N2	78.86(8)	N4–Ni1–N2	96.91(8)
O2–Ni1–O7	87.66(7)	N1–Ni1–O7	96.33(7)
N4–Ni1–O7	92.45(7)	N2–Ni1–O7	93.10(7)
O2–Ni1–N3	92.45(8)	N1–Ni1–N3	92.72(7)
N4–Ni1–N3	78.47(8)	N2–Ni1–N3	87.95(8)

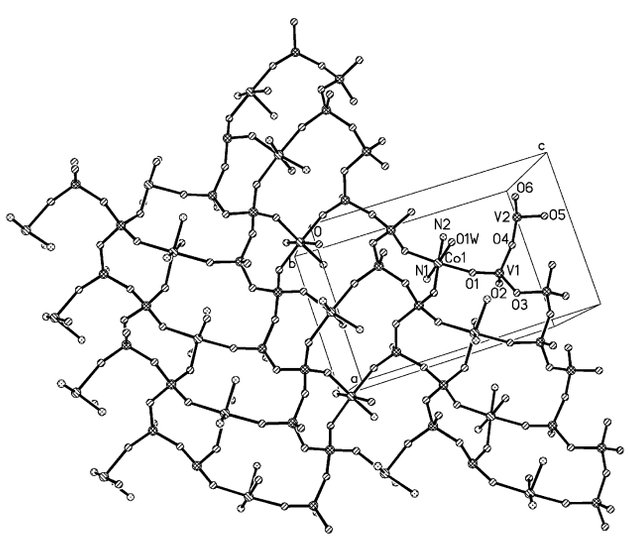

Fig. 2 The structure of **3** viewed along the *b*-axis and exhibiting the layer composed of 4,6-net sheets. All the C and H atoms are omitted for clarity.

structed from 2D deformed honeycomb layers where the basic structural unit appears to be a four-membered ring defined by Ni1V1V2V3 (Fig. 3, Table 4). Six adjacent such kind of units

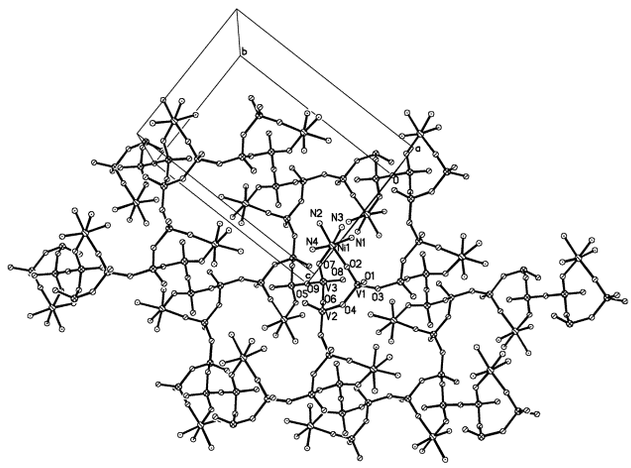

Fig. 3 The structure of **2** viewed along the *a*-axis showing its characteristic 2D deformed honeycomb layer structure. All the C and H atoms are omitted for clarity.

are bridged by O3, O9 and their symmetry equivalents to form a hexagon, which shares edges with another six neighboring hexagons so that a honeycomb structure is constructed. Interestingly, this deformed honeycomb layer displays a beautiful sinusoidal wave with an amplitude of about 13 Å and a period of about 15 Å when viewed down the *c*-axis, this pronounced characteristic has already been described in the structure of $Zn(bipy)_2V_6O_{17}$.[2a]

The nickel atom, which is in a distorted octahedral environment, is coordinated by four N atoms from two 2,2′-bipy ligands and two oxygen atoms from vanadium oxides, which adopt a *cis*-orientation. The Ni–N and Ni–O bond distances (average 2.081 and 2.054 Å, respectively) are comparable with those of **1** (average 2.064 Å for Ni–N and 2.062 Å for Ni–O bond distances). Each vanadium atom is coordinated by four oxygen atoms to form a VO_4 tetrahedral geometry, and the terminal vanadyl (V=O) group is found in all three crystallographically independent vanadium sites. The V2=O5 bond distance [1.577(2) Å] is slightly shorter than V1=O1 [1.6065(16) Å] and V3=O8 [1.610(2) Å], and also slightly shorter than V1=O2 in **1** [1.608(2) Å].

Magnetic properties of 1 and 2

Plots of $\chi_M T$ *vs.* T for **1** and **2** are shown in Figs. 4 and 5, respectively.

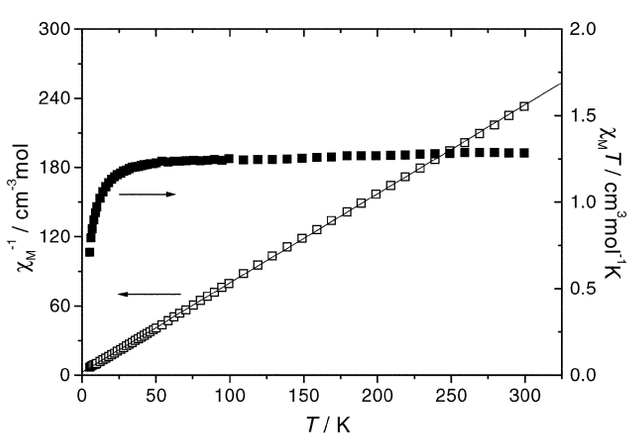

Fig. 4 Plots of $\chi_M T$ and χ_M^{-1} *vs.* T for **1**. The solid line represents the best fit to the Curie–Weiss law.

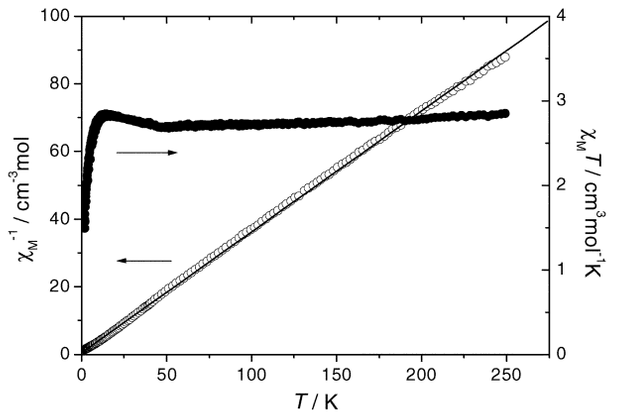

Fig. 5 Plots of $\chi_M T$ and $\chi_M{}^{-1}$ *vs.* T for **2**. The solid line represents the best fit to the Curie–Weiss law.

Complex 1. The $\chi_M T$ value at 300 K is *ca.* 1.28 cm^3 K mol^{-1} (3.2 μ_B), slightly higher than that (1.0 cm^3 K mol^{-1}, 2.83 μ_B) of an isolated Ni^{2+} ion ($S = 1$, $g = 2.0$) with diamagnetic V^{5+} ions ($S = 0$). As the temperature decreases, the $\chi_M T$ value decreases slowly until 55 K and then sharply falls to a minimum value of 0.71 cm^3 K mol^{-1} (2.38 μ_B) at 5.0 K. Such magnetic behavior is characteristic of the combination of zero-filed splitting of Ni^{2+} in an axially distorted octahedral environment and a weak antiferromagnetic interaction between Ni^{2+} ions. The magnetic susceptibility obeys the Curie–Weiss law [$\chi_M = 1/(T - \theta)$] in the whole range of 5–300 K, giving a Weiss constant $\theta = -3.3$ K, and a Curie constant $C = 1.29$ cm^3 K mol^{-1}, corresponding to a g value of 2.27.

Complex 2. At 250 K, the $\chi_M T$ value is *ca.* 2.84 cm^3 K mol^{-1} (4.77 μ_B), larger than that (2.0 cm^3 K mol^{-1}, 4.0 μ_B) of two isolated spin only Ni^{2+} ions ($S = 1$, $g = 2.0$) with a diamagnetic V^{5+} ion ($S = 0$). As the temperature decreases the $\chi_M T$ value decreases regularly until 47 K and then increases slightly before decreasing again. The magnetic susceptibility obeys the Curie–Weiss law in the whole range of 2–250 K with a Weiss constant $\theta = -1.3$ K, and a Curie constant, $C = 2.80$ cm^3 K mol^{-1}, corresponding to a g value of 2.38. The decrease and increase in $\chi_M T$ at high temperature and below 47 K might be contributed to the competition between zero-field splitting effects of axially distorted Ni^{2+} and very weak ferromagnetic coupling among distantly separated Ni^{2+} ions. The overall behavior of **2** suggests a dominant single ion effect with only very weak magnetic interactions.

The different coupling nature between Ni^{2+} ions in complexes **1** and **2** might be due to the different Ni ··· Ni separations in **1** and **2**. The shorter Ni–Ni distance *via* an –O–V–O– pathway (5.413 Å) in **1** might favor antiferromagnetic superexchange coupling, and the longer distance –O–V–O–V–O– pathway (9.750 Å) in **2** might be apt for a very weak ferromagnetic dipole–dipole interaction.[12]

Acknowledgements

This work was supported by the Visiting Scholar Foundation of Key Lab. in University (sponsored by the Education Ministry of China), the National Science Fund for Distinguished Young Scholars, and the State Key Project for Fundamental Research (G1998061305).

References

1 (*a*) P. J. Hagrman, D. Hagrman and J. Zubieta, *Angew. Chem., Int. Ed.*, 1999, **38**, 2638; (*b*) G. Centi, F. Trifro, J. R. Ebbner and V. M. Franchetti, *Chem. Rev.*, 1988, **88**, 55.
2 (*a*) Y. Zhang, J. R. D. DeBord, C. J. O'Connor, R. C. Haushalter, A. Clearfield and J. Zubieta, *Angew. Chem., Int. Ed. Engl.*, 1996, **35**, 989; (*b*) Y. Zhang, P. J. Zapf, L. M. Meyer, R. C. Haushalter and J. Zubieta, *Inorg. Chem.*, 1997, **36**, 2159; (*c*) J. R. D. DeBord, Y. Zhang, R. C. Haushalter, J. Zubieta and C. J. O'Connor, *J. Solid State Chem.*, 1996, **122**, 251.
3 (*a*) Z. Shi, L.-R. Zhang, G.-S. Zhu, G.-Y. Yang, J. Hua, H. Ding and S.-H. Feng, *Chem. Mater.*, 1999, **11**, 3565; (*b*) L.-R. Zhang, Z. Shi, G.-Y. Yang, X.-M. Chen and S.-H. Feng, *J. Chem. Soc., Dalton Trans.*, 2000, 275.
4 L.-M. Zheng, J.-S. Zhao, K.-H. Lii, L.-Y. Zhang, Y. Liu and X.-Q. Xin, *J. Chem. Soc., Dalton Trans.*, 1999, 939.
5 S. Aschwanden, H. W. Schmalle, A. Reller and H. R. Oswald, *Mater. Res. Bull.*, 1993, **28**, 45.
6 (*a*) a) X.-M. Zhang, M.-L. Tong and X.-M. Chen, *Chem. Commun.*, 2000, 1817; (*b*) C.-M. Liu, S. Gao and H.-Z. Kou, *Chem. Commun.*, 2001, 1670; (*c*) C.-M. Liu, S. Gao, H.-M. Hu and Z.-M. Wang, *Chem. Commun.*, 2001, 1636; (*d*) C.-M. Liu, Y.-L. Hou, J. Zhang and S. Gao, *Inorg. Chem.*, 2002, **41**, 140.
7 J. Gopalakrishnan, *Chem. Mater.*, 1995, **7**, 1265.
8 O. Kahn, *Molecular Magnetism*, VCH Publishers, New York, 1993.
9 P. J. Hagrman and J. Zubieta, *Inorg. Chem.*, 2000, **39**, 5218.
10 G. M. Sheldrick, SHELX 97, PC Version, University of Göttingen, 1997.
11 B.-Q. Ma, S. Gao, G. Su and G.-X. Xu, *Angew. Chem., Int. Ed.*, 2001, **40**, 434.
12 H.-H. Song, L.-M. Zheng, C.-H. Lin, S.-L. Wang, X.-Q. Xin and S. Gao, *Chem. Mater.*, 1999, **11**, 2382.